Opt Quant Electron (2012) 43:49–58
DOI 10.1007/s11082-011-9502-7

Saturable and reverse saturable absorption in aqueous silver nanoparticles at off-resonant wavelength

Misha Hari · S. Mathew · B. Nithyaja · Santhi Ani Joseph · V. P. N. Nampoori · P. Radhakrishnan

Received: 5 July 2011 / Accepted: 2 November 2011 / Published online: 27 November 2011

Abstract Silver nano-colloid was prepared by chemical reduction method and its nonlinear absorption properties were investigated by using open aperture z-scan experiment with nanosecond laser pulses operating at 532 nm. Interestingly, a switch over from saturable absorption to reverse saturable absorption was observed when the input intensity is increased from 28.1 to 175.8 MW/cm^2. The underlying mechanism responsible for the observed switching behaviour is the interplay between ground state plasmon band bleaching and excited state absorption. Theoretical fitting was done by using a model in which nonlinear absorption coefficient as well as saturation intensity are incorporated.

Keywords Silver nanocolloid · Surface plasmon resonance · Z-scan · Third order optical nonlinearity · Saturable absorption · Reverse saturable absorption · Two-photon absorption

1 Introduction

Research on noble metal nanoparticles has recently received considerable attention, because of their potential applications in photonic devices due to their large nonlinear susceptibilities and fast response time (Gurudas et al. 2008). Among the nanoparticles of noble metals, silver (Ag) and gold have received special interest, as they exhibit surface plasmon resonance (SPR) band in the visible region of the electromagnetic spectrum. The origin of this absorption band is attributed to the collective oscillations of the free electrons, in the conduction band near the Fermi level, caused by the interaction with the electromagnetic field. SPR absorption band can be tuned across the entire visible spectrum by varying the size and shape of the nanoparticles. The plasmon resonance of metal nanoparticles can cause local field enhancement and leads to many interesting properties. This enables them to find many applications such

M. Hari (✉) · S. Mathew · B. Nithyaja · S. A. Joseph · V. P. N. Nampoori · P. Radhakrishnan
International School of Photonics, Cochin University of Science and Technology, Cochin-22, India
e-mail: mishahari@cusat.ac.in

S. Mathew · P. Radhakrishnan
CELOS, Cochin University of Science and Technology, Cochin-22, India

as optical limiting, plasmon waveguide, sensor protection, medicine and nanoprobes (Elim et al. 2006; Shipway et al. 2000; Storhoff et al. 2004; West et al. 2003; Gao et al. 2007; Wang et al. 2005; Lapotko 2009; Francois et al. 2000).

The nonlinear optical properties of metal nanoparticles are strongly dependent on their size, shape as well as the dielectric medium (Lee et al. 2009; Link and El-Sayed 2003). In particular, the third order optical nonlinearity of metal nanoparticles and their nanocomposites has received a lot of attention (Ispasoiu et al. 2000; Philip and Kumar 2000; Smith et al. 1999; Boni et al. 2008; Zhang et al. 2003; Gomez et al. 2007; Gao et al. 2003; Ganeev et al. 2004). Z-scan technique is commonly adopted for the investigation of third order nonlinear optical properties of these materials. Z-scan is a single-beam method developed by Sheik Bahe el al. to measure the nonlinear absorption and nonlinear refraction of a thin material (Sheik-Bahe et al. 1990). Nonlinear absorption refers to the change in transmittance of a material as a function of intensity or fluence. There are variety of processes leading to nonlinear absorption like, two-photon absorption (TPA), multiphoton absorption, excited state absorption (ESA), free-carrier absorption (FCA), reverse saturable absorption (RSA) and saturable absorption (SA). RSA leads to increase in absorption in the sample with increase in intensity whereas, for SA, absorption in the sample decreases with increase in the input intensity.

It has been reported earlier that, metal nanoparticles exhibits a switch over behavior from SA to RSA when parameters like laser energy, particle-size and shape are changed (Gurudas et al. 2008; Elim et al. 2006; Lee et al. 2009; Gao et al. 2005; Deng et al. 2008; Karthikeyan et al. 2005; Karavanskii et al. 2004; Unnikrishnan et al. 2003; Anija et al. 2003; Zheng et al. 2010). For example, Gurudas et al. studied the picosecond optical nonlinearity in silver nanodots prepared by pulsed laser deposition at 532 nm (Gurudas et al. 2008). They observed a flip over from SA to RSA behavior at higher input irradiance. Similar kind of nonlinear optical absorption behavior is previously observed in Au/Ag coreshells (Anija et al. 2003), Au–Ag alloy nanoclusters (Philip and Kumar 2000), Au nanorods (Elim et al. 2006), Au nanocubes and nano-octahedra (Lee et al. 2009) and platinum nanoparticles (Gao et al. 2005) depending on the intensity of the incident radiation. Saturable absorption is attributed to the ground state plasmon bleach due to intraband electron excitation at moderate input intensities, while RSA at higher input intensities is attributed to various processes like, transient absorption from free carriers and photoejection of electrons, two photon absorption, nonlinear scattering etc.

In this paper, we report the nonlinear absorption characteristics of well dispersed and stable aqueous silver nano-colloids by open aperture z-scan measurements at 532 nm. It is observed that the sample acts as a saturable absorber and reverse saturable absorber at the same wavelength depending on the excitation intensity. Saturable absortion is attributed to the ground state bleaching at relatively low intensities and, RSA at high excitation intensities is ascribed to the cumulative effect of ESA, two photon absorption and nonlinear scattering. The intensity dependent switching behavior attributed by SA and RSA of noble metal nanoparticles can be possibly utilized for variety of photonic applications like optical pulse compression, mode locking, all-optical switching and optical power limiter (Gurudas et al. 2008; 1986; Ganeev et al. 2004, 2009; Kiran et al. 2004; Wang et al. 2010).

2 Experimental

Silver nanoparticles were prepared by chemical reduction of silver nitrate ($AgNO_3$) with sodium boro hydride ($NaBH_4$) in the presence of trisodium citrate (Jana et al. 2001). Trisodium citrate acts as a stabilizing agent. The preparation of the Ag nanoparticles is described briefly as follows. First, a 20 ml solution containing 0.25 mM $AgNO_3$ and 0.25 mM trisodium

citrate in water was prepared. While stirring vigorously, 0.6 ml of 10 mM $NaBH_4$ was added all at once. Then the color of the solution turned to yellow, indicating the formation of silver nanoparticles. The absorption spectrum of the sample was recorded by a UV/Vis spectrophotometer. The average size of the Ag nanoparticles obtained using Scanning Tunnelling Electron Microscopy (STEM).

The nonlinear optical absorption of aqueous solution of silver nanoparticles was investigated by open aperture z-scan. The advantage of z-scan measurement is that, it can separate the intensity dependent SA and RSA spatially. A Q-switched Nd:YAG laser (Spectra Physics LAB-1760, 532 nm, 7 ns, 10 Hz) was used as the light source. The laser beam was focused on the sample by a lens of focal length 200 mm. The radius of the beam ω_0 was calculated to be 42.5 μm. The Rayleigh length, $z0 = \pi\omega_0^2/\lambda$, was estimated to be 1.07 cm, which is much greater than the thickness of the sample cuvette (1 mm), and is an essential prerequisite for z-scan experiments. The sample cuvette was fixed on a computer-controlled translation stage, so that it could be accurately moved through the focal region of the laser beam over a length of 60 mm. The transmitted beam energy, reference beam energy and the ratios were measured simultaneously using an energy ratio meter (Rj7620, Laser Probe Corp.) having two identical pyroelectric detector heads (Rjp735). The detected signals were acquired, stored and processed by the computer.

3 Results and discussion

The size of the Ag nanoparticles was obtained using STEM as shown in Fig. (1). It can be seen that the nanoparticles are of spherical shape and the diameter of the particles falls in the range 2–10 nm as evident from the particle size distribution graph (Fig. 2). Absorption spectrum of the aqueous solution of silver nanoparticles is shown in Fig. (3). The SPR peak is observed at 402 nm. We performed open aperture z-scan of the Ag nano-colloid at different input energies. The experimental results at different peak intensities in the range $28 - 175\,\mathrm{MW/cm^2}$ are shown in Figs. (4)–(10). The sample exhibited interesting excitation intensity dependent behaviors. Saturation absorption behavior is observed when the excitation fluence was $28\,\mathrm{MW/cm^2}$ (Fig. 4). Figure (5) shows the nonlinear behaviour of the nanoparticles at a higher intensity, $40.4\,\mathrm{MW/cm^2}$ in which two symmetrical humps flanking a small valley is appeared around the focal point. As the power increased further, the depth of the valley increases. For example, when the input intensity is at $40.4\mathrm{MW/cm^2}$ the depth of the valley is 2.3 and at intensity $149.4\,\mathrm{MW/cm^2}$ the depth increases to 0.3. However, it is observed that at $175\,\mathrm{MW/cm^2}$, valley depth again reduced to 1.05. Thus by varying the input intensity in the range 28–175 $\mathrm{MW/cm^2}$, the sample exhibited SA as well as RSA behavior. Such a changeover in the sign of nonlinearity can be generally modelled by defining a nonlinear absorption coefficient $\alpha(I)$ which is a sum of independent positive and negative transmissioon coefficients (Gao et al. 2005). To interpret the flip of SA around the beam waist, we combine the SA coefficeint and the TPA coefficient to yield the total absorption coefficient as,

$$\alpha(I) = \frac{\alpha_0}{1 + I/I_s} + \beta I \tag{1}$$

where the first term describes negative nonlinear absorption such as SA, and the second term describes positive nonlinear absorption such as RSA and two photon absorption. α_0 is the linear absorption coefficient, I is the laser intensity, and I_s is the saturation intensity. β is the positive nonlinear absorption coefficient. Then the normalised transmittance is given by,

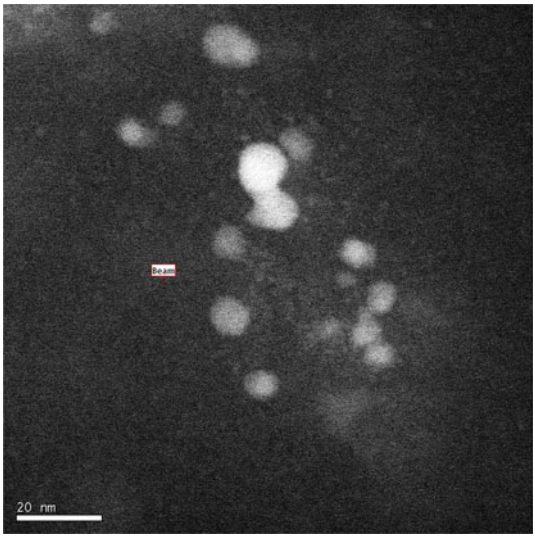

Fig. 1 STEM image of the silver nanoparticles

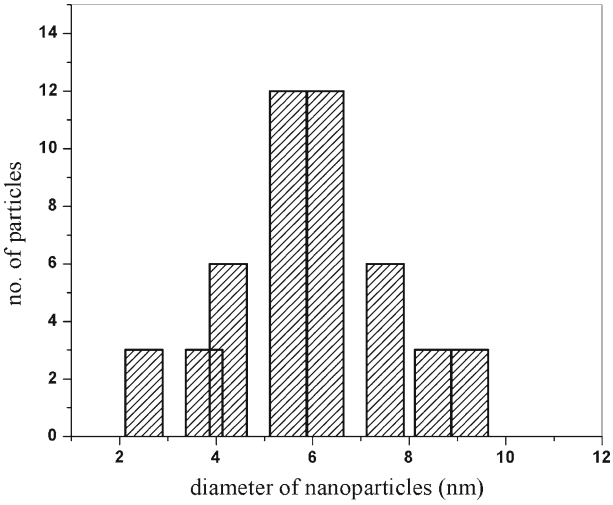

Fig. 2 Size distribution of silver nanoparticles

$$T(z) = \sum_{m=0}^{\infty} \frac{\left[\frac{-\alpha I_0 L_{eff}}{1+z^2/z_0^2}\right]^m}{(m+1)} \tag{2}$$

where $L_{eff} = (1 - e^{-\alpha 0^L})/\alpha_0$, z is the longitudinal displacement of the sample from the focus (z = 0), α is the nonlinear absorption coefficient, I_0 is the on axis peak intensity at the focus, L_{eff} is the effective interaction length, L is the sample length, z_0 is the Rayleigh diffraction length. Theoretical fit of the experimental data could be done by substituting Eq. (1) into Eq .(2). It can be seen from Figs. (4)–(9) that the theoretical fitting is in good agreement with the experimental data. The estimated values of saturation intensity and nonlinear absorption coefficient β are given in Table 1.

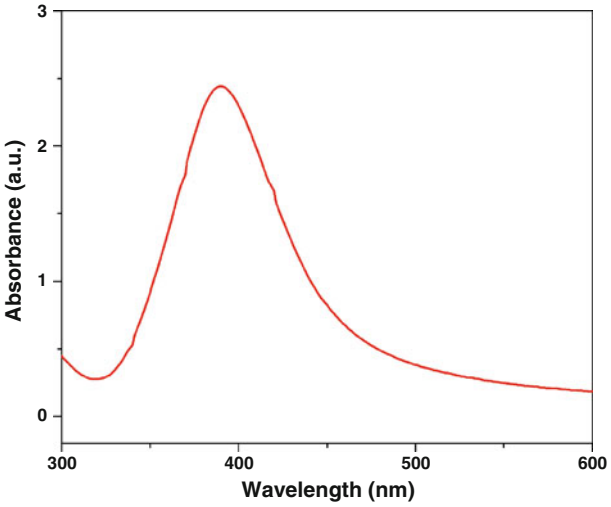

Fig. 3 Absorption spectrum of aqueous silver nanoparticles

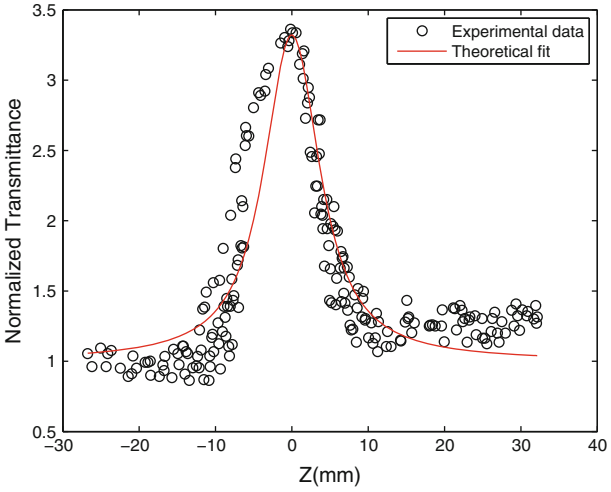

Fig. 4 Open-aperture z-scan *curve* of aqueous silver nanoparticles at 532 nm at laser beam intensity, $I_0 = 28.1\,\mathrm{MW/\,cm^2}$

Optical properties of metal nanoparticles are influenced by the localized outermost electrons in the d-bands and by quasi-free-electrons in the s-p conduction band. Nonlinear Optical properties of noble metals in the visible range basically originate from two mechanisms, namely interband and intraband transtions. The interband transition arises between the levels in the d-band that are just below the Fermi level and the conduction band, whereas intraband transition happens from ground state to the excited state in the conduction band. Electrons are firstly pumped from ground state to the excited state where they then become free carriers (SPR absorption), this process is subsequently followed by the broad band absorption of these free carriers (free carrier absorption). Then finally the excited electrons relax to the ground state by electron-electron coupling, electron phonon interaction and phonon–phonon

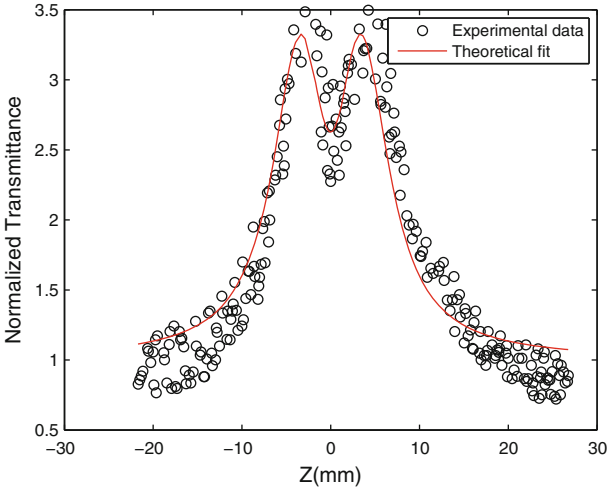

Fig. 5 Open-aperture z-scan *curve* of aqueous silver nanoparticles at 532 nm at laser beam intensity, $I_0 = 40.4\,\text{MW/ cm}^2$

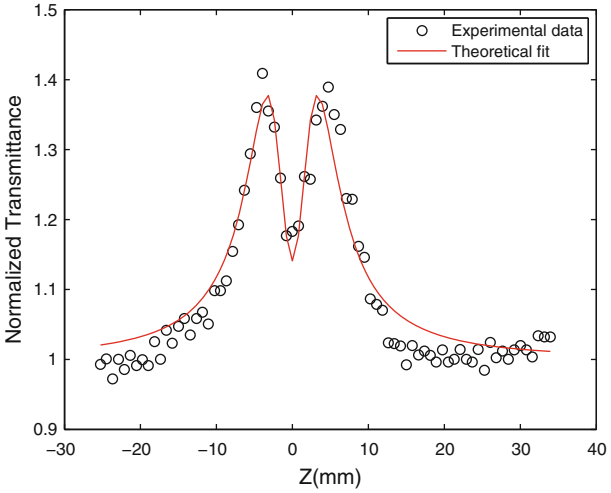

Fig. 6 Open-aperture z-scan *curve* of aqueous silver nanoparticles at 532 nm at laser beam intensity, $I_0 = 61.5\,\text{MW/ cm}^2$

relaxation (Zheng et al. 2010; Venkatram et al. 2006). A simple scheme of the possible absorption and relaxation mechanisms is shown in Fig. (10) (Gurudas et al. 2008).

When the sample is far from the focus, the weak intensity cannot induce any nonlinearity and the transmittance is unity. As the sample is moved towards the focus, the moderate intensity induces the plasmon oscillation of the electrons within the conduction band. Thus majority of the nanoparticles are pumped to the excited state, leading to a smaller population of the ground state. This causes the bleaching in the ground state plasmon absorption band. At this intensity level, the transmitted intensity will be maximum resulting in saturation absorption (SA) behavior (hump). When the sample approaches the focal point, intensity

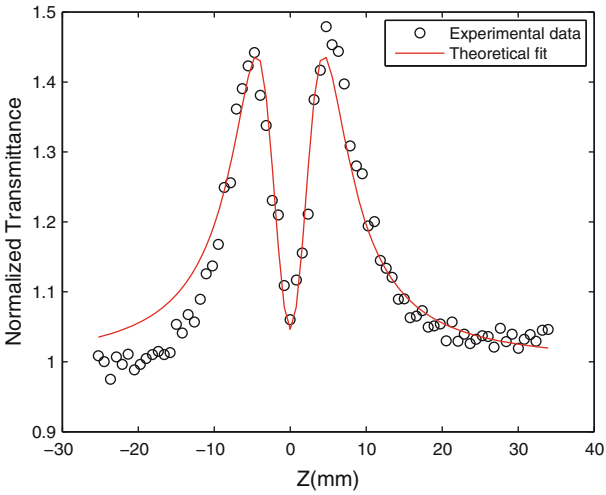

Fig. 7 Open-aperture z-scan *curve* of aqueous silver nanoparticles at 532 nm at laser beam intensity, $I_0 = 87.9\,\mathrm{MW/cm^2}$

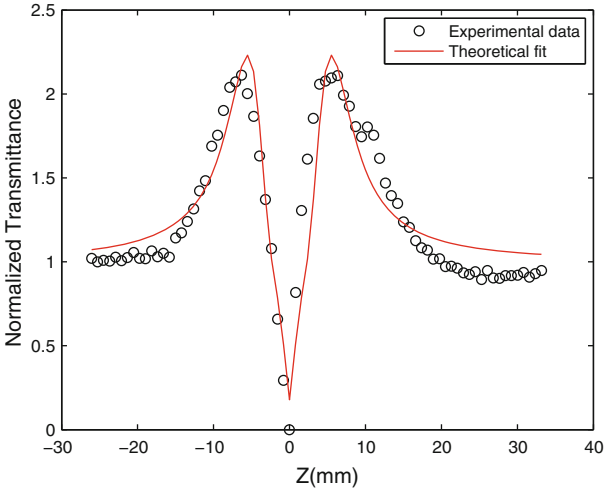

Fig. 8 Open-aperture z-scan *curve* of aqueous silver nanoparticles at 532 nm at laser beam intensity, $I_0 = 149.4\,\mathrm{MW/cm^2}$

Table 1 The saturation intensities and the nonlinear absorption coefficients obtained by theoretical fitting of experimental data at different laser intensities I_0

I_0 (MW/cm^2)	I_s (MW/cm^2)	β (cm/MW)
28.1	32.1	−2.562
40.4	30.1	9.116
61.5	66.0	2.425
87.9	96.9	1.727
149.4	130.0	2.013
175.8	182.6	0.4659

increases further and the nonlinear absorption begins to play a dominant role. This intensity is sufficient enough to pump the free carriers in the conduction band to higher energy levels by ESA. As a result, transmittance decreases to a minimum at the focal point and a valley

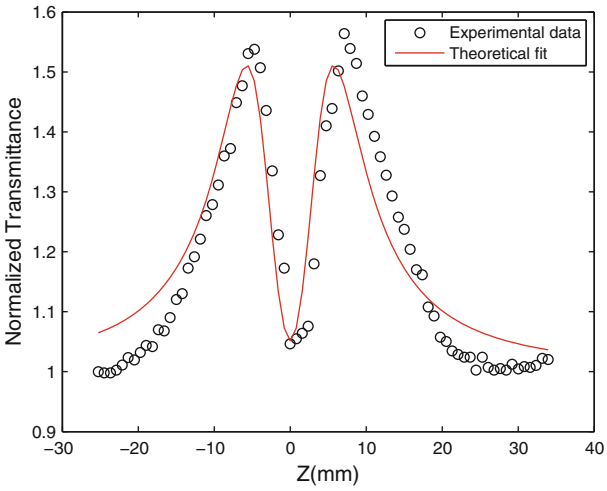

Fig. 9 Open-aperture z-scan *curve* of aqueous silver nanoparticles at 532 nm at laser beam intensity, $I_0 = 175.8\,\mathrm{MW/cm^2}$

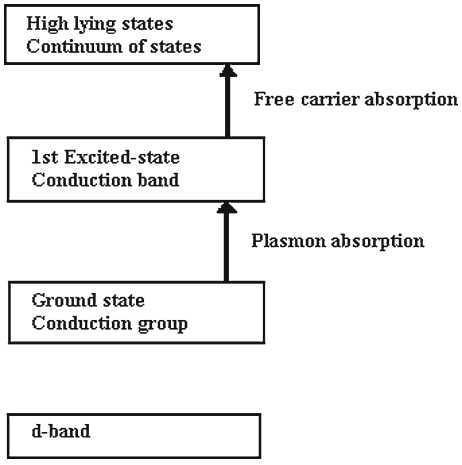

Fig. 10 Energy-level diagram explaining the processes leading to SA and RSA

appears in the open aperture z-scan curves. In the case of silver, electronic transition between d-bands and conduction band requires photon energies larger than 4 eV (Gurudas et al. 2008). In the present experiment, the excitation wavelength is 532 nm (2.33 eV), which is much less than the interband transition threshold. Thus the observed nonlinearity is mainly due to intraband transition at moderate input intensities. However, at high input fluencies, we cannot discard the possibility of TPA in addition to the FCA. As the wavelength range of interband transition in Ag is located below 320 nm, the TPA connected with interband transition can be excited with 532 nm radiation at high intensity (Philip and Kumar 2000; Zheng et al. 2008). Another possible mechanism which is responsible for the observed RSA behavior at high excitation intensities is the nonlinear scattering (Lee et al. 2009). However, further experimental investigation is required to find out the contribution from nonlinear scattering in the observed RSA behavior. We speculate that the RSA behavior at high excitation intensities is a cumulative effect of ESA, TPA and nonlinear scattering.

Similar switching behaviors have also been previously observed for silver nanowires/silica gel glass composite (Zheng et al. 2010), Au:SiO_2, Ag:ZrO_2 (Anija et al. 2003), platinum

nanoparticles (Gao et al. 2005) and silver nanoparticles in PMMA (Deng et al. 2008), under nanosecond irradiation at 532 nm. Different reasonings are given in the literature to explain the observed behavior. In the case of silver nanowires/silica gel nanocomposite, an underlying mechanism for this switch over behavior was proposed from the viewpoint of the different environments and electronic dynamics of silver nanowires in liquid and solid-state matrices. For Au:SiO_2 and Ag:ZrO_2, the observed behavior is explained in terms of electronic Kerr nonlinearity and nonlinear light scattering.

Interestingly, in the present experiment, a switch over behavior from SA to RSA is observed for silver nanoparticles of sizes ranges from 2 to 10 nm under excitation with nanosecond pulses at 532 nm wavelength when the input intensity was at 40.4 MW/cm^2. This intensity threshold for the switching behavior is substantially low compared to the previous results (Gao et al. 2005; Deng et al. 2008; Anija et al. 2003; Zheng et al. 2010).

4 Conclusions

In summary, silver nano-colloid was prepared by chemical reduction method and its nonlinear absorption properties have been studied using open aperture z-scan at excitation wavelength 532 nm. The nano-colloid exhibited a switch over from SA to RSA as the excitation intensity is increased. The SA behavior is attributed to the ground state plasmon band bleaching and RSA is attributed to the cumulative effect of ESA, TPA and nonlinear scattering.

Acknowledgments The authors acknowledge University Grants Commission for financial assistance. Author MH would like to thank Kerala State Council for Science Technology and Environment for providing Research fellowship.

References

Anija, M., Thomas, J., Singh, N., Nair, A.S., Tom, R.T., Pradeep, T., Philip, R.: Nonlinear light transmission through oxide-protected Au and Ag nanoparticles: an investigation in the nanosecond domain. Chem. Phys. Lett. **380**, 223–229 (2003)

Band, Y.B., Harter, D.J., Bavli, R.: Optical pulse compressor composed of saturable and reverse saturable absorbers. Chem. Phys. Lett. **126**, 280–284 (1986)

Boni, L.D., Wood, E.L., Toro, C., Hernandez, F.E.: Optical saturable absorption in gold nanoparticles. Plasmonics **3**, 171–176 (2008)

Deng, Y., Sun, Y., Wang, P., Zhang, D., Jiao, X., Ming, H., Zhang, Q., Jiao, Y., Sun, X.: Nonlinear optical properties of silver colloidal solution by in situ synthesis technique. Curr. Appl. Phys. **8**, 13–17 (2008)

Elim, H.I., Yang, J., Lee, J.Y.: Obseration of saturable and reverse-saturable absorption at longitudinal surface plasmon resonance in gold nanorods. Appl. Phys. Lett. **88**, 083107 (2006)

Francois, L., Mostafavi, M., Belloni, J., Delouis, J.F., Delaire, J., Feneyrou, P.: Optical limitation induced by gold clusters 1 size effect. J. Phys. Chem. B **104**, 6133–6137 (2000)

Gao, Y., Chang, Q., Ye, H., Jiao, W., Li, Y., Wang, Y., Song, Y., Zhu, D.: Size effect of optical limiting in gold nanoparticles. J. Phys. Chem. **336**, 99–102 (2007)

Gao, Y., Wang, Y., Song, Y., Li, Y., Qu, S., Liu, H., Dong, B., Zu, J.: Strong optical limiting property of a novel silver nanoparticle containing C60 derivative. Opt. Commun. **223**, 103–108 (2003)

Gao, Y., Zhang, X., Li, Y., Liu, H., Wang, Y., Chang, Q., Jiao, W., Song, Y.: Saturable absorption and reverse saturable absorption in platinum nanoparticles. Opt. Commun. **251**, 429–433 (2005)

Ganeev, R.A., Ryasnyansky, A.I., Stepanov, A.L., Usmanov, T.: Saturated absorption and nonlinear refraction of silicate glasses doped with silver nanoparticles at 532 nm. Opt. Quantum Electron. **36**, 949–960 (2004)

Ganeev, R.A., Ryasnyansky, A.I., Stepanov, A.L., Usmanov, T.: Saturated absorption and nonlinear refraction of silicate glasses doped with silver nanoparticles at 532 nm. Opt. Quantum Electron. **36**, 949–960 (2004)

Ganeev, R.A., Tugushev, R.I., Usmanov, T.: Application of the nonlinear optical properties of platinum nanoparticles for the mode locking of Nd: glass laser. Appl. Phys. B **94**, 647–651 (2009)

Gomez, L.A., Araujo, C.B.D., Silva, A.M.B., Galembeck, A.: Influence of stabilizing agents on the nonlinear susceptibility of silver nanoparticles. J. Opt. Soc. Am. B **24**, 2136–2140 (2007)
Gurudas, U., Brooks, E., Bubb, D.M., Heiroth, S., Lippert, T., Wokaun, A.: Saturable and reverse saturable absorption in silver nanodots at 532 nm using picoseconds laser pulses. J. Appl. Phys. **104**, 073103 (2008)
Ispasoiu, R.G., Balogh, L., Varnavski, O.P., Tomalia, D.A., Goodson, T. III.: Large optical limiting from novel metal-dendrimer nanocomposite materials. J. Am. Chem. Soc. **122**, 11005–11006 (2000)
Jana, N.R., Gearheart, L., Murphy, C.J.: Wet chemical synthesis of silver nanorods and nanowires of controllable aspect ratio. Chem. Commun. **7**, 617–618 (2001)
Karthikeyan, B., Thomas, J., Philip, R.: Optical nonlinearity in glass-embedded silver nanoclusters under ultrafast laser excitation. Chem. Phys. Lett. **414**, 346–350 (2005)
Karavanskii, V.A., Simakin, A.V., Krasovskii, V.I., Ivanchenko, P.V.: Nonlinear optical properties of colloidal silver nanoparticles produced by laser ablation in liquids. Quantum Electron. **34**(7), 644–648 (2004)
Kiran, P.P., Bhaktha, B.N.S., Rao, D.N., De, G.: Nonlinear optical properties and surface plasmon enhanced optical limiting in Ag-Cu nanoclusters co-doped in SiO2 Sol-Gel Films. J. Appl. Phys. **96**, 6717–6723 (2004)
Lapotko, D.: Optical excitation and detection of vapor bubbles around plasmonic nanoparticles. Opt. Express **17**, 2538–2556 (2009)
Lee, Y.H., Yan, Y., Polavarapu, L., Xu, Q.H.: Nonlinear optical switching behavior of Au nanocubes and nano-octahedra investigated by femtosecond z-scan measurements. Appl. Phys. Lett. **95**, 023105 (2009)
Link, S., El-Sayed, M.A.: Optical properties and ultrafast dynamics of metallic nanocrystals. Annu. Rev. Phys. Chem. **54**, 331–366 (2003)
Philip, R., Kumar, G.R.: Picosecond optical nonlinearity in monolayer-protected gold, silver, and gold-silver alloy nanoclusters. Phys. Rev. B **62**, 13160–13166 (2000)
Shipway, A.N., Katz, E., Willner, I.: Nanoparticles arrays on surfaces for electronic optical and sensor applications. Chem. Phys. Schem. **1**, 18–52 (2000)
Sheik-Bahe, M., Said, A.A., Wei, T.-H., Hagan, D.J., Van Stryland, E.W.: Sensitive measurement of optical nonlinearities using a single beam. IEEE J. Quantum Electron. **26**, 760–769 (1990)
Smith, D.D., Yoon, Y., Boyd, R.W., Campell, J.K., Baker, L.A., Crooks, R.M., George, M.: Z-scan measurement of the nonlinear absorption of a thin gold film. J. Appl. Phys. **86**, 6200–6205 (1999)
Storhoff, J.J., Lucas, A.D., Garimella, V., Bao, Y.P., Muller, U.R.: Homogeneous detection of unamplified genomic DNA sequences based on colorimetric scatter of gold nanoparticle probes. Nat. Biotechnol. **22**, 883–887 (2004)
Unnikrishnan, K.P., Nampoori, V.P.N., Ramakrishnan, V., Umadevi, M., Vallabhan, C.P.G.: Nonlinear optical absorption in silver nanosol. J. Phys. D Appl. Phys. **36**, 1242–1245 (2003)
Venkatram, N., Santhosh Kumar, R.S., Rao, D.N., Medda, S.K., De, S., De, G.: Nonlinear optical absorption and switching properties of gold nanoparticle dopped SiO2—TiO2 sol gel films. J. Nanosci. Nanotechnol. **6**, 1990–1994 (2006)
Wang, K., Long, H., Fu, M., Yang, G., Lu, P.: Intensity dependent reversal of nonlinearity sign in a gold nanoparticle array. Opt. Lett. **35**, 1560–1562 (2010)
Wang, C., Yap, F.L., Zhang, Y.: Micropatterning of polystyrene nanoparticles and its bioapplications. Colloids Surf. B Biointerfaces **46**, 255–260 (2005)
West, R., Wang, Y., Goodson, T. III.: Nonlinear absorption properties in novel gold nanostructured topologies. J. Phys. Chem. B **107**, 3419–3426 (2003)
Zhang, P., Zhang, S., Li, J., Liu, D., Guo, Z.X., Ye, C., Zhu, D.: The self assembly of gold nanoparticles with C_{60} nanospheres: fabrication and optical limiting effect. Chem. Phys. Lett. **382**, 599–604 (2003)
Zheng, C., Ye, X.Y., Cai, S.G., Wang, M.J., Xiao, X.Q.: Observation of nonlinear saturable and reverse saturable absorption in silver nanowires and their silica gel glass composite. Appl. Phys. B. **101**, 835–840 (2010)
Zheng, C., Du, Y., Feng, M., Zhan, H.: Shape dependence of nonlinear optical behaviors of nanostructured silver and their silica gel glass composites. Appl. Phys. Lett. **93**, 143108 (2008)